



**HAL**  
open science

## Mesoscale modelling of water vapour in the tropical UTLS: two case studies from the HIBISCUS campaign

V. Marécal, Georges Durré, K. Longo, S. Freitas, Emmanuel D. Rivière,  
Michel Pirre

### ► To cite this version:

V. Marécal, Georges Durré, K. Longo, S. Freitas, Emmanuel D. Rivière, et al.. Mesoscale modelling of water vapour in the tropical UTLS: two case studies from the HIBISCUS campaign. *Atmospheric Chemistry and Physics Discussions*, 2006, 6 (4), pp.8241-8284. 10.5194/acp-7-1471-2007 . hal-00328005

**HAL Id: hal-00328005**

**<https://hal.science/hal-00328005>**

Submitted on 18 Jun 2008

**HAL** is a multi-disciplinary open access archive for the deposit and dissemination of scientific research documents, whether they are published or not. The documents may come from teaching and research institutions in France or abroad, or from public or private research centers.

L'archive ouverte pluridisciplinaire **HAL**, est destinée au dépôt et à la diffusion de documents scientifiques de niveau recherche, publiés ou non, émanant des établissements d'enseignement et de recherche français ou étrangers, des laboratoires publics ou privés.



Distributed under a Creative Commons Attribution 4.0 International License

**Water vapour  
modelling in the  
tropical UTLS**

V. Marécal et al.

# Mesoscale modelling of water vapour in the tropical UTLS: two case studies from the HIBISCUS campaign

V. Marécal<sup>1</sup>, G. Durrý<sup>2,3</sup>, K. Longo<sup>4</sup>, S. Freitas<sup>4</sup>, E. D. Rivière<sup>2</sup>, and M. Pirre<sup>1</sup>

<sup>1</sup>Laboratoire de Physique et Chimie de l'Environnement, CNRS and Université d'Orléans, 3A Avenue de la Recherche Scientifique, 45071 Orléans cedex 2, France

<sup>2</sup>Groupe de Spectroscopie Moléculaire et Atmosphérique, CNRS and Université de Reims, Moulin de la Housse, B.P. 1039, 51687 Reims Cedex, France

<sup>3</sup>Service d'Aéronomie, CNRS and Institut Pierre Simon Laplace, 91371 Verrières-le-Buisson Cedex, France

<sup>4</sup>Centro de Previsão de Tempo e Estudos Climáticos, Rodovia Presidente Dutra, km 40 SPRJ 12630-000, Cachoeira Paulista – SP, Brazil

Received: 12 May 2006 – Accepted: 10 July 2006 – Published: 29 August 2006

Correspondence to: V. Marécal (virginie.marecal@cnsr-orleans.fr)

Title Page

Abstract

Introduction

Conclusions

References

Tables

Figures

◀

▶

◀

▶

Back

Close

Full Screen / Esc

Printer-friendly Version

Interactive Discussion

## Abstract

In this study, we evaluate the ability of the BRAMS mesoscale model compared to ECMWF global analysis to simulate the observed vertical variations of water vapour in the tropical upper troposphere and lower stratosphere (UTLS). The observations are balloon-borne measurements of water vapour mixing ratio and temperature from micro-SDLA (Tunable Diode Laser Spectrometer) instrument. Data from two balloon flights performed during the 2004 HIBISCUS field campaign are used to compare with the mesoscale simulations and to ECMWF analysis.

The mesoscale model performs significantly better than ECMWF analysis for water vapour in the upper troposphere and similarly or slightly worse for temperature. The improvement provided by the mesoscale model for water vapour comes mainly from (i) the enhanced vertical resolution in the UTLS (250 m for BRAMS and ~1 km for ECMWF model) and (ii) the more detailed microphysical parameterization providing ice supersaturations as in the observations. The ECMWF vertical resolution (~1 km) is too coarse to capture the observed fine scale vertical variations of water vapour in the UTLS. In near saturated or supersaturated layers, the mesoscale model relative humidity with respect to ice saturation is close to observations provided that the temperature profile is realistic. For temperature, ECMWF analysis gives good results partly thanks to data assimilation. The analysis of the mesoscale model results showed that in undersaturated layers, the water vapour profile depends mainly on the dynamics. In saturated/supersaturated layers, microphysical processes play an important role and have to be taken into account on top of the dynamical processes to understand the water vapour profiles.

In the lower stratosphere, the ECMWF model and the BRAMS model give very similar water vapour profiles that are significantly dryer than micro-SDLA measurements. This similarity comes from the fact that BRAMS is initialised using ECMWF analysis and that no mesoscale process acts in the stratosphere leading to no modification of the BRAMS results with respect to ECMWF analysis.

## Water vapour modelling in the tropical UTLS

V. Marécal et al.

Title Page

Abstract

Introduction

Conclusions

References

Tables

Figures

◀

▶

◀

▶

Back

Close

Full Screen / Esc

Printer-friendly Version

Interactive Discussion

# 1 Introduction

It is known that the stratosphere is dry since Brewer (1949) who performed water vapour measurements with a balloon-borne frost-point hygrometer in England. This rather late discovery concerning a major air compound is related to the technical difficulty for measuring very low water vapour mixing ratios down to a few ppmv at low temperatures. In the low and mid-troposphere, humidity is operationally monitored through the radio-sounding network providing fairly accurate in situ measurements of water vapour with a fine vertical resolution. In the upper troposphere and the lower stratosphere (UTLS), it is known that the radio-sounding sensors generally used for measuring humidity are not reliable because of the low temperature conditions. This is even more critical in the tropics where temperature down to about  $-80^{\circ}\text{C}$  are generally found around the tropopause. Miloshevich et al. (2001), Fujiwara et al. (2003) and Turner et al. (2003) showed that the Vaisala RS80 radiosonde system, which is the most widely used, have a dry bias that increases with decreasing temperatures. Newer sondes (Vaisala RS90) that are fitted with a different humidity sensor are designed to provide more accurate humidity measurements at cold temperatures for the future operational network. The current operational monitoring from radiosondes is complemented by remote sensing observations from satellite instruments, mainly vertical and limb sounders, that provide a global coverage but with much coarser vertical and horizontal resolutions than radiosondes. Therefore, remote sensing observations do not allow the study of the fine scale processes affecting the vertical structure of the water vapour field within the UTLS.

On the research side, chiefly three types of instruments flown on aircraft or balloon platforms have proven their ability to provide in situ water vapour measurements in the UTLS with an inaccuracy within a few percents: Lyman- $\alpha$  hygrometers (e.g. Hintsa et al., 1999; Zöger et al., 1999), frost-point hygrometers (e.g. Ovarlez and Van Velthoven, 1997) and tunable diode laser spectrometers (e.g. May, 1998; Durry and Mégie 1999). The measurements obtained from these instruments showed a large vertical variability

## Water vapour modelling in the tropical UTLS

V. Marécal et al.

Title Page

Abstract

Introduction

Conclusions

References

Tables

Figures

◀

▶

◀

▶

Back

Close

Full Screen / Esc

Printer-friendly Version

Interactive Discussion

of the water vapour mixing ratio in the UTLS and also significant differences between measurements gathered at different latitudes and seasons (e.g. Ovarlez et al., 2000; Vömel et al., 2002; Offermann et al., 2002; Durry et al., 2002; Durry and Hauchecorne, 2005). The water vapour variability in the UTLS is related to the history of the air mass sampled at a given level that can be affected by both dynamical (long-range horizontal transport, vertical transport by convection, stratosphere-troposphere exchanges) and microphysical processes (mainly dehydration by ice nucleation, subsequent growth and sedimentation of the condensed particles). The understanding and the prediction of the water vapour distribution in the tropical upper troposphere is currently a key issue since this region is likely to control the entry of water vapour in the stratosphere.

The measurements available so far are not sufficient to provide a full picture of the relative impact of the different processes affecting the water vapour distribution in the tropics. The modelling approach can be used to complement these observations, in particular three-dimensional meteorological models that represent in a consistent manner the dynamical and microphysical processes affecting the water distribution. Global meteorological models, such as the ECMWF model, do not use a vertical resolution fine enough in the UTLS to resolve the observed small scale variability of humidity. Moreover, the parameterizations used in global models only include a limited number of microphysical processes. To overcome these weaknesses, a possible approach is to use a Lagrangian one-dimensional microphysical model along trajectories extracted from global analyses (Gettelman et al., 2002; Jensen and Pfister, 2004). Trajectories are generally interpolated from 4-daily analyses missing short-time or local variations of temperature that can impact on the microphysics. An alternative tool is the three-dimensional limited-area meteorological model, also called a mesoscale model, that can be run with a fine vertical resolution in the UTLS and that can account for a large number of microphysical processes. The time evolution of the microphysics being calculated at each model time step, the microphysics is always fully consistent with the model dynamics and thermodynamics. These models and their associated parameterizations are designed to provide realistic forecasts of tropospheric weather phenomena

**Water vapour  
modelling in the  
tropical UTLS**

V. Marécal et al.

Title Page

Abstract

Introduction

Conclusions

References

Tables

Figures

◀

▶

◀

▶

Back

Close

Full Screen / Esc

Printer-friendly Version

Interactive Discussion

that take place in the troposphere. However, specific processes occurring in the uppermost troposphere or lower stratosphere, such as sub-visible cirrus, may not be well captured by mesoscale models. Moreover, these models rely on global analyses for initial and boundary conditions that may be uncertain in the UTLS since few humidity observations are available for assimilation systems in this atmospheric layer.

In this context, the objective of this paper is to evaluate the potential benefit of using a mesoscale model compared to a global analysis to reproduce the vertical variations of water vapour in the tropical UTLS. For this purpose the temperature and water vapour profiles from mesoscale model simulations and from ECMWF analyses were compared to the measurements gathered by the micro-SDLA instrument during the balloon flights SF2 and SF4 launched during the HIBISCUS campaign. These two flights were performed in different meteorological conditions: SF2 ahead of a cold front event and SF4 nearby a strong convective system. HIBISCUS was a European funded project aiming at studying the air composition of the tropical UTLS and in particular its link with tropical convection. The main HIBISCUS field campaign took place during the wet season in February and March 2004 in Bauru (State of São Paulo in Brazil). This campaign was mainly based on balloon-borne measurements of chemical species and water vapour and complemented by modelling studies (Pommereau et al., 2006<sup>1</sup>). Using a trajectory analysis, Huret et al. (2006a<sup>2</sup>, b<sup>3</sup>, c<sup>4</sup> interpreted SF2 and SF4 flight data in detail. The present paper is a complementary study focused on the simulation of the water vapour

<sup>1</sup>Pommereau, J.-P., Garnier, A., Held, G., and the Hibiscus team: An overview of the HIBISCUS campaign, Atmos. Chem. Phys. Discuss., in preparation, 2006.

<sup>2</sup>Huret, N., Durry, G., Freitas, G., et al.: In situ laser diode measurements of H<sub>2</sub>O during the HIBISCUS campaign. Part 1: Intrusion of dry mid-latitude air in the tropical upper troposphere, Atmos. Chem. Phys. Discuss., in preparation, 2006a.

<sup>3</sup>Huret, N., Durry, G., Rivièrè, E. D., et al.: In situ laser diode measurements of H<sub>2</sub>O during the HIBISCUS campaign. Part 2: Investigation of the isentropic transport impact on the TTL water vapor content, same issue, in preparation, 2006b.

<sup>4</sup>Huret, N., Durry, G., Rivièrè, E. D., et al.: In situ laser diode measurements of H<sub>2</sub>O during the HIBISCUS campaign. Part 3: Investigation of convective event impact on the TTL water

## Water vapour modelling in the tropical UTLS

V. Marécal et al.

Title Page

Abstract

Introduction

Conclusions

References

Tables

Figures

◀

▶

◀

▶

Back

Close

Full Screen / Esc

Printer-friendly Version

Interactive Discussion

distribution in the UTLS by a mesoscale model.

In Sect. 2, SF2 and SF4 flights are shortly described together with their meteorological environment. The water vapour measurements from micro-SDLA instrument are presented in Sect. 3. The BRAMS mesoscale model used in this study and the simulation setup is described in Sect. 4 together with a brief recall of ECMWF analysis characteristics. The results are analysed in Sect. 5 and conclusions are given in Sect. 6.

## 2 SF2 and SF4 flightS

### 2.1 SF2 flight and its meteorological environment

The SF2 balloon was launched from Bauru, Brazil (22.36° S, 49.02° W) at 20:18 UTC (17:02 local time) on 13 February 2004. The balloon reached a maximum altitude of 20 km at sunset (22:11 UTC). Then the balloon experienced 3 h of slow night time descent down to 11.8 km where it was cut down. The trajectory of the balloon is shown in Fig. 1.

During the afternoon of 13 February 2004, the Bauru radar observations showed that there was a moderate convective activity around Bauru with several weak convective cells developing within the radar range (240 km). During the balloon flight, a 300 km-length rainband associated with a cold front was moving eastward towards Bauru. The rainband reached Bauru around 07:00 UTC on 14 February, long after the end of the balloon flight. The balloon track was always located east of this rainband. The meteorological situation is illustrated in Fig. 2a from the accumulated rainfall estimated by the Tropical Rainfall Measuring Mission (TRMM, <http://trmm/gsfc.nasa.gov>) between 19:30 UTC on 13 February and 10:30 UTC on 14 February.

vapor content, same issue, in preparation, 2006c.

Title Page

Abstract

Introduction

Conclusions

References

Tables

Figures

⏪

⏩

◀

▶

Back

Close

Full Screen / Esc

Printer-friendly Version

Interactive Discussion

## 2.2 SF4 flight and its meteorological environment

The SF4 balloon was launched from Bauru at 20:13 UTC on 24 February 2004. The balloon reached a maximum altitude of 20.2 km shortly before sunset followed by 45 min float and a slow descent (starting at 21:57 UTC) down to 10.7 km where it was cut down. The trajectory of the balloon is shown in Fig. 1.

Late in the afternoon on 24 February 2004, a strong convective system developed to the north west of Bauru and moved towards the Bauru city. It reached Bauru soon after the flight launch. This system is located at the south edge of a very large area of convection covering most of central Brazil. The situation is illustrated in Fig. 2b by the accumulated TRMM rainfall between 24 February at 16:30 UTC and 25 February at 04:30 UTC.

## 3 Micro-sdla measurements

### 3.1 Description of micro-sdla instrument

The micro-SDLA sensor is a balloon borne near-infrared diode laser spectrometer that yields in situ measurements of H<sub>2</sub>O, CH<sub>4</sub> and CO<sub>2</sub> in the UTLS by absorption spectroscopy (description found in Durrý et al., 2004). Three InGaAs laser diodes emitting respectively at 1.39  $\mu\text{m}$  (H<sub>2</sub>O), 1.60  $\mu\text{m}$  (CO<sub>2</sub>) and 1.65  $\mu\text{m}$  (CH<sub>4</sub>) are connected with optical fibers to a multipass optical cell operated open to the atmosphere that provides a 28 m absorption path length. The laser beams are absorbed in situ by the ambient molecules as it is propagated between both mirrors of the optical cell and in situ absorption spectra are recorded at the cell output using a direct-differential detection technique. The amount of absorbed laser energy is then related to the molecular concentration using the Beer-Lambert Law, in situ pressure and temperature measurements and an adequate molecular model (Durrý and Megie, 1999). The atmospheric pressure is obtained from an onboard Paroscientific Inc baratron gauge with an inaccuracy

Title Page

Abstract

Introduction

Conclusions

References

Tables

Figures

◀

▶

◀

▶

Back

Close

Full Screen / Esc

Printer-friendly Version

Interactive Discussion

**Water vapour  
modelling in the  
tropical UTLS**

V. Marécal et al.

Title Page

Abstract

Introduction

Conclusions

References

Tables

Figures

◀

▶

◀

▶

Back

Close

Full Screen / Esc

Printer-friendly Version

Interactive Discussion

of  $\sim 0.01$  hPa. Three meteorological thermistors (VIZ Manufacturing Company) located at different places in the gondola, are used to measure in situ the temperature with a precision of 1K. Regarding water vapor, the instrument provides a dynamical range for the measurements of four orders of magnitude that permits to measure continuously  $\text{H}_2\text{O}$  in the troposphere and the TTL despite the large difference in the  $\text{H}_2\text{O}$  amounts observed in both regions of the atmosphere (Durry and Megie, 2000). For the flights discussed in this paper, the temporal resolution was of one  $\text{H}_2\text{O}$  concentration sample per second for SF2 and was upgraded to four samples per second for the second flight, SF4. The  $\text{H}_2\text{O}$  molecular mixing ratio was retrieved from the absorption spectra with a non-linear least-squares fit to the full molecular line shape and by using our set of revisited molecular parameters, i.e.  $\text{H}_2\text{O}$  line strengths and pressure-broadening coefficients from Parvitte et al. (2002) and Durry et al. (2005). The measurement error in the  $\text{H}_2\text{O}$  concentration measurements ranges from 5% to 10%. A complete description of the retrieval process and associate sources of errors is found in Durry and Megie (1999) and Durry et al. (2002). For HIBISCUS, the micro-SDLA was operated in an unattended manner without telemetry- telecommand from small open balloons inflated with  $3000 \text{ m}^3$  of Helium to probe the troposphere and the TTL. The spectra were stored onboard and processed after the flights. The reported  $\text{H}_2\text{O}$  data gathered in the UTLS, were recorded as usual at nighttimes during the slow descent of the gondola to prevent pollution of the measurement by water vapor outgassing from the balloon envelope (Durry and Megie, 2000; Durry et al., 2004). The  $\text{H}_2\text{O}$  data in the troposphere were obtained under parachutes after cut-off from the flight chain (Durry et al., 2004).

### 3.2 SF2 water vapour and temperature profiles

For the SF2 flight analysis, we make use of the  $\text{H}_2\text{O}$  data yielded by the micro-SDLA in the altitude region ranging from 18.5 km altitude and after sunset (22:45 UTC) down to 4.6 km altitude (00:46 UTC) during its descent.

The water vapour mixing ratio (noted  $r_v$  hereafter) and the temperature profiles from micro-SDLA are shown in Figs. 3a and b. Note that there were no data between

12 774 and 13 385 km altitude because of technical problems. The water vapour profile (Fig. 3a) shows a large variability below 10 km altitude with a dry layer between 5 and 7 km. Above 10 km, there is a decrease with altitude up to an hygropause at 17 km altitude reaching  $\sim 3$  ppmv with enhanced variability between 14 and 17 km. Above 17 km,  $r_v$  tendency is to increase slowly with altitude. The temperature profile (Fig. 3b) decreases with altitude up to the cold point tropopause ( $-78.8^\circ\text{C}$ ) at 15.5 km altitude. Above 15.5 km, there is a large variability of the temperature profile with a tendency to slowly increase with altitude. Figure 3c depicts the relative humidity with respect to ice in % (RHI) calculated from the measured temperatures and  $r_v$ . To allow a fair comparison with the model results (Sect. 5), the calculation of RHI is based on the formula of the saturation pressure with respect to ice used in the BRAMS model which provides RHI values close within  $\pm 0.5\%$  to those found using Sonntag (1998)'s formula. The RHI profile shows that the air is very close to saturation or supersaturated between 10 and 16 km altitude. The very large supersaturation values up to  $\text{RHI}=190\%$  are consistent with the water vapour data presented in Ovarlez et al. (2000), Ovarlez et al. (2002) and Jensen et al. (2005a, b). The two layers where very large super-saturations occur (around 13.5 and around 15.5 km altitude) are associated with enhanced water vapour mixing ratios. This indicates that, in these layers, the excess of water vapour has not been removed yet at the time of the measurements by ice nucleation and subsequent sedimentation of the condensed particles. Nevertheless, there are favourable conditions for the air to dehydrate within the following hours.

### 3.3 SF4 water vapour and temperature profiles

For the SF4 flight analysis, we use  $\text{H}_2\text{O}$  data achieved during the descent of the sensor in the altitude region ranging from 18.7 km (24 February at 22:21 UTC) down to 3.6 km (25 February at 00:48 UTC).  $r_v$ , temperature and RHI profiles for the SF4 flight are shown in Fig. 4. One important feature in Fig. 4a is the very dry layer around 9 km with values below 100 ppmv. The  $r_v$  profile also exhibits relative minima of water vapour around 15 km and 16.7 km altitude. The temperature profile decreases fairly

## Water vapour modelling in the tropical UTLS

V. Marécal et al.

Title Page

Abstract

Introduction

Conclusions

References

Tables

Figures

◀

▶

◀

▶

Back

Close

Full Screen / Esc

Printer-friendly Version

Interactive Discussion

monotonically up to 14.5 km altitude. Above there are significant variations with altitude with an absolute minimum of  $-78.8^{\circ}\text{C}$  at 18.1 km. The measured profile is supersaturated up to 15 km altitude with the exception of the very dry layer between 8.5 and 10 km (see Fig. 4c). In this very dry layer, RHI reaches values below 10%. Typical supersaturations are around  $\text{RHI}=125\%$  with peaks up to 195%. The supersaturated layers are analysed in Huret et al. (2006b)<sup>3</sup> using microphysical measurements from microlidar instruments obtained during the flight (Di Donfrancesco et al., 2005). Note that the water vapour profiles and the temperature profiles above 15 km for the SF2 and SF4 flights are significantly different. This is related to the different meteorological conditions in which the two profiles were measured.

## 4 Modelling tools

### 4.1 Mesoscale model and simulation setup

The regional model used in this study is the BRAMS (Brazilian Regional Atmospheric Modeling System, <http://www.cptec.inpe.br/brams>). BRAMS is a new version of the RAMS (Walko et al., 2000) tailored to the tropics. The BRAMS/RAMS model is a multipurpose numerical prediction model designed to simulate atmospheric circulations spanning in scale from hemispheric scales down to large eddy simulations of the planetary boundary layer. Among the additional possibilities of BRAMS compared to RAMS version 5.04 are the ensemble version of shallow cumulus and deep convection parameterizations (Grell and Devenyi 2002, Freitas et al., 2005), new 1 km vegetation data for South America, heterogeneous soil moisture assimilation procedure (Gevaerd and Freitas, 2006) and SIB2.5 surface parameterization. The cloud microphysics is the single moment bulk scheme from Walko et al. (1995) which includes five categories of ice: pristine ice crystals, snow, aggregates, graupel and hail.

A BRAMS simulation was performed for each flight in order to analyse the model ability to simulate the observed temperature and water vapour profiles (called reference

Title Page

Abstract

Introduction

Conclusions

References

Tables

Figures

◀

▶

◀

▶

Back

Close

Full Screen / Esc

Printer-friendly Version

Interactive Discussion

simulation hereafter). The reference simulation for both flights is similar except for the initial time/date of the simulation. The simulation starts on 12 February 2004 at 00:00 UTC for SF2 and on 23 February 2004 at 00:00 UTC for SF4 and lasts 60 h for both flights. The reference run includes one grid centred on Bauru. The domain dimension is  $2800 \times 2400 \text{ km}^2$  (see domain plotted in Fig. 2) and is chosen to include the large scale dynamic fluxes that can possibly affect the water vapour profiles for both flights. Because of the fairly large domain extension we chose 20 km horizontal grid-spacing. The vertical coordinate is a terrain-following height coordinate extending from the surface to 30 km altitude with a 250 m grid-spacing between 13 and 20 km altitude (total number of levels=74). The initial conditions are from the ECMWF operational analysis. The BRAMS fields are constrained at the boundaries by Newtonian relaxation (nudging) with the 6-hourly ECMWF operational analyses. The initial soil moisture and soil temperature are derived from the assimilation of TRMM accumulated rainfall estimates. The parameterizations of sub-grid scale shallow and deep convection are used.

Four sensitivity simulations were also run to test the impact on the results of the horizontal and vertical resolutions and the microphysical scheme. The setup of these simulations is explained in Sect. 5 together with the corresponding analysis of the results.

## 4.2 ECMWF analysis

Operational analysis produced at ECMWF (European Centre for Medium-range Weather Forecasts) are used in this study. One major characteristic of these analyses is that it includes the stratosphere up to the 1 hPa level. At the date of the HIBISCUS campaign, ECMWF model had 60 vertical levels and a T511 truncation. ECMWF fields used are extracted on a  $0.5^\circ \times 0.5^\circ$  grid. The assimilation system is a four-dimensional variational system including data over 12 h windows. For humidity, the data assimilated are the specific humidity profiles from radiosondes below 300 hPa, surface relative hu-

### Water vapour modelling in the tropical UTLS

V. Marécal et al.

Title Page

Abstract

Introduction

Conclusions

References

Tables

Figures

◀

▶

◀

▶

Back

Close

Full Screen / Esc

Printer-friendly Version

Interactive Discussion

midity and satellite radiances including moisture sensitivity.

## 5 Model results

### 5.1 Comparison of the reference run and ECMWF analysis with SF2 measurements

The comparison between micro-SDLA SF2 measurements and the ECMWF analysis is shown in Fig. 5 and the comparison between micro-SDLA SF2 measurements and the BRAMS reference run is shown in Fig. 6. The micro-SDLA data are averaged vertically in Fig. 5 (resp. Fig. 6) to match the ECMWF (resp. BRAMS reference run) vertical grid. To plot the ECMWF results, we have selected the profile the closest to the SF2 descent mean location plus the 8 profiles around from the 14 February 00:00 UTC analysis fields. To plot the BRAMS reference simulation results, we have selected the profile closest to the SF2 descent mean location plus all the profiles around as far as 60 km from this profile from hourly outputs between 22:00 UTC on 13 February 2004 and 01:00 UTC on 14 February 2004. This time interval corresponds approximately to the descent duration. Note that in the 13–20 km layer where the BRAMS vertical resolution is 250 m (29 levels), there are only 8 ECMWF model levels corresponding to ~1 km vertical spacing. Statistical results comparing model and observations are given in Table 1. For the statistical analysis, RHI results were preferred to  $r_v$  results to evaluate the water vapour model performance since  $r_v$  values cover several orders of magnitude and therefore statistics for  $r_v$  would be weighted towards the large  $r_v$  at low altitudes. The correlation for temperature is not given since it is greater than 0.999 for all model configurations.

Figure 5 and Fig. 6 show that the main water vapour and temperature features observed by micro-SDLA in the UTLS are largely smoothed when averaged on the ECMWF vertical grid while they are still present when averaged on the BRAMS reference run grid. ECMWF analysis does not reproduce the observed variations in the UTLS. This is related to the vertical resolution which only allows the simulation of

## Water vapour modelling in the tropical UTLS

V. Marécal et al.

Title Page

Abstract

Introduction

Conclusions

References

Tables

Figures

◀

▶

◀

▶

Back

Close

Full Screen / Esc

Printer-friendly Version

Interactive Discussion

**Water vapour  
modelling in the  
tropical UTLS**

V. Marécal et al.

Title Page

Abstract

Introduction

Conclusions

References

Tables

Figures

◀

▶

◀

▶

Back

Close

Full Screen / Esc

Printer-friendly Version

Interactive Discussion

structures having a vertical extension greater than a few kilometres. Below 10 km, the ECMWF analysis exhibits a dry layer but moister than the mean microSDLA profile below 8 km. From 12 km upwards, ECMWF analysis generally underestimates  $r_v$ , particularly above 15 km altitude. The dry bias of ECMWF analysis in the upper troposphere was already pointed out in several studies (e.g. Ovarlez and Van Velthoven, 1997; Ovarlez et al., 2000; Spichtinger et al., 2005). In the stratosphere, ECMWF water vapour analysis field is nearly constant since no humidity data are available for assimilation. For the temperature (Fig. 5b), there is a generally good agreement between micro-SDLA and ECMWF analysis within 2 K. In particular, ECMWF analysis exhibits a well-defined minimum of temperature at the cold point tropopause similar to micro-SDLA. In Fig. 5c, the ECMWF RHI profile shape is qualitatively similar to observations as illustrated by a RHI correlation of 0.905. Quantitatively, ECMWF RHI is close to the observations mainly below 10 km leading to a fairly large value of RMSE (26.5%). Note that there are no ECMWF RHI values greater than 100%. This illustrates the fact that supersaturated states with respect to ice are not allowed below a temperature of  $-23^\circ\text{C}$  in the ECMWF model. Therefore, it is not possible in ECMWF analysis to reproduce the observed supersaturated layers in the UTLS. Moreover, because water vapour is removed instantaneously as condensed water below  $-23^\circ\text{C}$  when super-saturated with respect to ice, ECMWF generally underestimates  $r_v$  compared to observations.

As illustrated in Fig. 6a, the reference simulation provides  $r_v$  profiles that are in better agreement with the observations than ECMWF analysis. The model simulates the dry layer below 10 km altitude but not as dry as in the observations, similarly to ECMWF analysis. In this altitude range, the SF2 balloon was flown in a transition region between a dry and a moist air mass where the water vapour gradient is strong. The difference between the model and the observations indicates that the model dynamics has driven slightly too early the moist air mass associated to the front towards the Bauru area. The zigzag shape found in the observations in this layer is also not reproduced by the mesoscale model. The reason is that there is for any model variable a correlation between vertical levels, particularly between two adjacent levels. Therefore

the model cannot simulate a vertical structure with an alternation of minima and maxima on adjacent levels. In the 10–14 km layer, the reference run shows a very good agreement with micro-SDLA measurements. In the 14–17.3 km range, the S-shape of the mean micro-SDLA profile is reproduced by the model but with less pronounced minima. Above 17.5 km altitude, the model gives nearly constant values for  $r_v$  with a low variability between the selected profiles as in ECMWF analysis. For temperature (see Fig. 6b), the reference simulation is generally in good agreement with the measurements (RMSE=1.84 K) except near the cold point tropopause level where the local sharp minimum is not simulated by the model. There is a  $\sim 5$  K difference at 15.5 km altitude. As shown in Fig. 5b, this minimum is present in ECMWF analysis. The information on this important feature does not appear in the ECMWF 48 h forecast started on 12 February at 00:00 UTC. It is brought in the 14 February 00:00 UTC analysis by the assimilation of observations. This indicates that the precursor information leading to this feature was not present in the 12 February 00:00 UTC ECMWF analysis used as initial state for the BRAMS simulations. More generally, the analysis gives better statistics than the forecast (see Table 1) thanks to data assimilation.

The general shape of the observed RHI profile in Fig. 6c is reproduced by the model (RHI correlation=0.960 and RHI RMSE=15.7%) except around 15.5 km and 13.5 km altitude where the model does not provide the observed large supersaturations and above 17.3 km where the model is significantly dryer. Unlike ECMWF analysis, BRAMS microphysical scheme allows supersaturations with respect to ice at a given temperature. The threshold for the ice supersaturation in the model is 100% for the relative humidity with respect to liquid water. For the tropical UTLS conditions, this constraint leads to large possible model ice supersaturations as illustrated in Fig. 6c (green dashed line). This means that observed large ice supersaturations can be simulated by BRAMS leading to a slower removal of water vapour by ice nucleation than in ECMWF model. This is illustrated by the generally greater values of  $r_v$  simulated by BRAMS in the 12–17 m layer compared to ECMWF analysis leading to a better agreement with micro-SDLA. This indicates that there is a significant influence of the microphysical

**Water vapour  
modelling in the  
tropical UTLS**

V. Marécal et al.

Title Page

Abstract

Introduction

Conclusions

References

Tables

Figures

◀

▶

◀

▶

Back

Close

Full Screen / Esc

Printer-friendly Version

Interactive Discussion

scheme on the water vapour mixing ratios in the upper troposphere.

Figures 5 and 6 show that the BRAMS simulation provides generally better results for SF<sub>2</sub> than the ECMWF analysis. These improvements are possibly related to the enhanced BRAMS vertical resolution but also to the finer horizontal resolution and the more detailed microphysical parameterization.

In order to test the impact of the vertical resolution on the BRAMS model performances, a sensitivity simulation was performed with a 1 km resolution in the UTLS (~ECMWF vertical resolution) instead of the 250 m resolution in the reference run. Statistical results in Table 1 show that the sensitivity run provides results for temperature similar to ECMWF analysis and a RHI mean profile significantly closer to the observations than ECMWF analysis. This means that with a similar vertical resolution BRAMS performs similarly to ECMWF analysis for temperature but significantly better for water vapour. Note that it is not pertinent to compare the statistics of the sensitivity run to those of the reference run since (i) they are calculated over a smaller number of points because of the different vertical grid spacing used and (ii) they correspond to an averaged profile in which the small scale structures are largely smoothed.

To test the importance of the horizontal resolution on the mesoscale model results two sensitivity tests were run. In the first one, we used a 50 km resolution (~ECMWF horizontal resolution) in BRAMS instead of 20 km. The corresponding statistics that are given in Table 1 show that using a 50 km horizontal resolution leads to results only slightly deteriorated compared to the reference simulation: 1.8% difference on the RHI RMSE. The second sensitivity simulation was run with two nested grids. The outer grid is the reference run grid (20 km horizontal resolution) and the inner grid is centred on Bauru and has a 5 km horizontal resolution. For the 5 km grid, the convection parameterization is not used. The water vapour statistics for this run are better (RHI RMSE=13.2%) than for the reference run (RHI RMSE=15.7) while results for temperature are slightly deteriorated. The analysis of the two sensitivity runs shows the impact on water vapour of a finer horizontal resolution in this case is positive. This is because using a finer resolution provides a more accurate simulation of small scale features and

## Water vapour modelling in the tropical UTLS

V. Marécal et al.

Title Page

Abstract

Introduction

Conclusions

References

Tables

Figures

◀

▶

◀

▶

Back

Close

Full Screen / Esc

Printer-friendly Version

Interactive Discussion

their associated microphysics.

In summary, the mesoscale model performs better than ECMWF analysis in predicting the observed SF<sub>2</sub> water vapour and RHI profiles. The BRAMS model provides improved dynamics by using finer vertical and horizontal resolutions but also a more realistic representation of the microphysical processes.

## 5.2 Analysis of the reference run for SF<sub>2</sub> flight

In this section, we analyse the model results in order to identify the processes leading to the modelled temperature and humidity profiles and to understand the model behaviour compared to the observations. This study being focused on the UTLS we will restrict this analysis to the results above 10 km altitude. Within the UTLS (meaning here above 10 km) it is possible to identify the TTL (tropical tropopause layer) which is the transitional layer between air with tropospheric properties and air with stratospheric properties (Highwood and Hoskins, 1998; Folkins et al., 1999). The issue of how to define the TTL is not settled. Here, the TTL will be defined as in Huret et al. (2006b)<sup>3</sup>: the base is the chemopause and the top is where the lapse rate reaches  $2 \text{ K km}^{-1}$ , i.e. stratospheric conditions. Using this definition we found that the model predicts a TTL extending from 13.7 to 17.3 km. A similar analysis was done using the SF<sub>2</sub> micro-SDLA temperatures by Huret et al. (2006b)<sup>3</sup>. They found that the observed TTL is between 13.8 and 18.2 km altitude. Thus, the model predicts a TTL base in agreement with micro-SDLA measurements while the TTL top in the model is slightly lower than the observations. The model does not provide the sharp temperature minimum around 15.5 km but a fairly smooth transition between negative and positive lapse rates.

A trajectory analysis is used to diagnose the processes that lead to the modelled water vapour and temperature profiles. Backward trajectories were calculated from the model outputs along the SF<sub>2</sub> descent locations using the methodology proposed by Freitas et al. (2000) which takes into account the subgrid effects of wet convective processes. The results of this method are reliable providing that the modelled convective precipitation is well located. This point is checked by comparing the TRMM accumu-

## Water vapour modelling in the tropical UTLS

V. Marécal et al.

Title Page

Abstract

Introduction

Conclusions

References

Tables

Figures

◀

▶

◀

▶

Back

Close

Full Screen / Esc

Printer-friendly Version

Interactive Discussion

lated rainrate (Fig. 2a) to the model accumulated rainrate (Fig. 7a). The comparison shows that the model precipitation field is qualitatively consistent with the observations. Only backward trajectories over 12 h are used since the analysis performed here is limited to the processes that occur just before the flight measurements.

From the trajectory analysis three layers were identified. Their characteristics are given in Table 2. In layer 1 (10–13.7 km), the model predicts very accurately both temperature and RHI profiles except for the thin layer of supersaturated air observed in the 13.5–14 km altitude range (Fig. 6c). This particular layer will be discussed in more details below together with the analysis of layer 2. Between 10 and 12.8 km, the good model consistency with micro-SDLA shows that the model is able to simulate the dynamical and microphysical processes that lead to the observed  $r_v$  and T. The trajectory analysis indicates that in layer 1 the air is lifted by the dynamics associated with the front located west of Bauru and experiences the formation of large amounts of ice particles possibly leading to a significant removal of water vapour. To test the impact of the ice microphysical process on water vapour a sensitivity simulation was run with simplified microphysics in which the water vapour can only be condensed as liquid cloud water where supersaturation with respect to liquid water occurs (i.e. no ice particles can be produced). For the sensitivity run displayed in Fig. 8,  $r_v$  mean profile in layer 1 is greater by about a factor of 1.4 on average compared to the reference run. This large difference comes from the ice formation/growth and the consecutive dehydration by sedimentation which are not taken into account in the simplified microphysics run. This indicates that it is necessary to include this process to obtain a realistic water vapour profile.

In layer 2 (TTL, 13.7–17.3 km), the trajectory analysis showed that the air slowly rises due to radiative warming. Between 13.5 and 14.3 km, the trajectory analysis indicates that significant ice formation occurred during the previous 12 h leading to progressive dehydration. At the time of the flight, this layer is still slightly supersaturated meaning that the ice nucleation process is still in progress and that more dehydration could occur after. The large peaks of supersaturation observed around 13.5 km and

**Water vapour  
modelling in the  
tropical UTLS**

V. Marécal et al.

Title Page

Abstract

Introduction

Conclusions

References

Tables

Figures

◀

▶

◀

▶

Back

Close

Full Screen / Esc

Printer-friendly Version

Interactive Discussion

**Water vapour  
modelling in the  
tropical UTLS**

V. Marécal et al.

Title Page

Abstract

Introduction

Conclusions

References

Tables

Figures

◀

▶

◀

▶

Back

Close

Full Screen / Esc

Printer-friendly Version

Interactive Discussion

around 15.5 km (Fig. 6c) are not reproduced by the model which produces too warm temperatures (Fig. 6b) at these altitudes. The water vapour field being linked to temperature conditions in particular when close to saturated conditions, it is important to evaluate the possible impact of the model temperature overestimation on the water vapour field. For this purpose, RHI was recalculated using the model  $r_v$  profile and micro-SDLA temperatures instead of the model temperatures. The result displayed in Fig. 6c (green solid line) shows that if the BRAMS model had simulated more realistic temperatures in these two layers it would have lead to larger ice supersaturations and thus to a much better agreement with micro-SDLA RHI profile, particularly for the layer around 15.5 km altitude.

In layer 3 (above 17.3 km), the BRAMS model predicts significantly drier conditions and consistent temperatures compared to micro-SDLA measurements. In this layer, the model produces a stratospheric water vapour field very close to ECMWF analysis. This is because no small or meso-scale processes occur. Indeed, the water vapour distribution in this layer is mainly driven by large scale horizontal fluxes since (i) vertical motions are weak and there is no convective overshooting in the BRAMS domain and (ii) no microphysical processes occur because air is largely undersaturated.

In summary, simulation results showed that microphysical processes play an important role in the distribution of water vapour and an appropriate parameterization allowing supersaturation with respect to ice is needed to model observed  $r_v$  profiles. In near saturated or supersaturated layers it is necessary to simulate realistic temperatures since microphysical processes are extremely temperature dependent.

### 5.3 Comparison of the reference run and ECMWF analysis with SF4 measurements

For SF4, the comparison between micro-SDLA and ECMWF analysis (resp. reference run) is displayed in Fig. 9 (resp. Fig. 10). We used ECMWF analysis at 00:00 UTC on 25 February 2004 and BRAMS outputs from 22:00 UTC on 24 February 2004 to 01:00 UTC on 25 February 2004.

Figure 9a shows that ECMWF analysis  $r_v$  is generally dryer than the micro-SDLA  $r_v$

mean profile for all altitudes except in the very dry layer located around 9 km which is well captured by the ECMWF analysis. For temperature (Fig. 9b), the ECMWF analysis is consistent with microSDLA measurements within 1 K. The ECMWF RHI profile (Fig. 9c) reproduces the general shape of the observations (RHI correlation=0.801) but is characterised by largely lower values (RMSE=48.5%) compared to microSDLA RHI except in the dry layer. There is hardly any supersaturation with respect to ice in the ECMWF analysis in the layers 3.5–8 m and 10–15 km. As for SF2, ECMWF analysis underestimates water vapour in the upper troposphere (above 10 km). This is partly because water vapour is immediately converted into ice when supersaturation with respect to ice occurs below  $-23^{\circ}\text{C}$ . Another reason for the poor accuracy of ECMWF water vapour analysis in the UTLS is the few humidity data that are used in the assimilation system. Nevertheless, ECMWF analysis (14 February 00:00 UTC) is better than the 48 h forecast started on 12 February at 00:00 UTC as illustrated by the statistics given in Table 3.

As shown in Figs. 10a and b, the main water vapour and temperature variations observed by micro-SDLA in the UTLS (TTL) are kept when averaged on the BRAMS reference run grid. Comparing Fig. 9 to Fig. 10 shows that the reference run performs generally better than ECMWF analysis for RHI and water vapour except in the dry layer and slightly worse for temperature with respect to micro-SDLA observations. In Fig. 10a, the mesoscale model produces a dry layer around 10 km altitude but significantly too moist compared to micro-SDLA observations and ECMWF analysis and located about 1 km higher. In the reference run, the SF4 flight track at the altitude of the dry layer is located in a transition zone associated with a large  $r_v$  gradient as illustrated by the large variability of the selected model profiles around the SF4 flight track in this layer. This transition zone is oriented north-west/south-east and located between the moist convection zone south of the transition zone and the dry intrusion of low stratosphere mid-latitude air ( $\sim 100$  ppmv) north of the transition zone as analysed by Huret et al. (2006a)<sup>2</sup>. In the ECMWF analysis the SF4 flight track is located within the dry intrusion and gives more realistic results for the dry layer. The compar-

**Water vapour  
modelling in the  
tropical UTLS**

V. Marécal et al.

Title Page

Abstract

Introduction

Conclusions

References

Tables

Figures

◀

▶

◀

▶

Back

Close

Full Screen / Esc

Printer-friendly Version

Interactive Discussion

ison between the reference simulation and microSDLA measurements indicates that the reference simulation forecasts the dry intrusion too far from the SF4 flight location shifted by about 150 km. Below this layer, the reference run  $r_v$  profile is dryer than micro-SDLA. Above 12 km the model  $r_v$  is consistent with the measurements up to 16.8 km altitude. The micro-SDLA step shape structure is reproduced by the model although shifted in altitude by about 0.5 km. Above 16.8 km, the model is significantly dryer than the observations and exhibits very limited variations. Figure 10b shows that the temperature is well simulated in the reference run (RMSE=1.26 K) although the fine scale variations between 14.7 and 18 km are not produced by the model. For RHI (Fig. 10c), the model reproduces the general shape (RHI correlation=0.797) with generally significantly lower values (RMSE for RHI ~30%).

As previously done for SF2, a sensitivity test was performed using a 1 km vertical resolution similar to ECMWF model to evaluate the impact of the vertical resolution on the reference simulation performance and to allow a possible comparison to ECMWF analysis. The corresponding results are given in Table 3. When using a 1 km vertical resolution, the BRAMS simulation RHI profile is significantly closer to the observations (RMSE=35.9%) than ECMWF analysis (RMSE=48.5%). This is the contrary for temperature with values of RMSE of 1.19 K for the BRAMS and 0.80 K for ECMWF analysis. This means that for SF4 ECMWF analysis is better for temperature compared to BRAMS with a similar vertical resolution. In Table 3 are also given the statistics for the ECMWF 48h forecast started on 12 February 2004, i.e. having the same initial state as the BRAMS simulations. Temperature RMSE for the ECMWF 48 h forecast is similar to the mesoscale simulation with 1 km vertical resolution. This indicates that the good performance of the ECMWF analysis for temperature comes from the data assimilation. For RHI, the analysis statistics are poor but better than the 48 h forecast statistics also thanks to data assimilation.

The importance of the horizontal resolution is evaluated using two test simulations with 50 km and 5 km horizontal resolutions. Results of these sensitivity tests are fairly similar to the reference simulation as shown by the statistics given in Table 3. Contrarily

**Water vapour  
modelling in the  
tropical UTLS**

V. Marécal et al.

Title Page

Abstract

Introduction

Conclusions

References

Tables

Figures

◀

▶

◀

▶

Back

Close

Full Screen / Esc

Printer-friendly Version

Interactive Discussion

to SF2, there is no significant improvement probably because the water vapour profile is mainly driven by large scale dynamics for this case study.

In summary, the ECMWF analysis and the BRAMS simulations give good results for temperature and significantly underestimate on average RHI although the BRAMS model performs better. Compared to SF2, SF4 statistical results are slightly better for temperature ( $\sim 1.2$  K RMSE for SF4 and  $\sim 1.7$  K for SF2) but worse for RHI ( $\sim 30\%$  RMSE for SF4 and  $\sim 16\%$  for SF2) and consequently for  $r_v$ . This indicates that the BRAMS water vapour performance depends on the considered meteorological situation. In particular, the model is not able to simulate the very sharp gradient of water vapour: e.g. in SF4 the transition between the dry layer and the supersaturated layer just above.

#### 5.4 Analysis of the reference run for SF4 flight

In this section we analyse in more details the BRAMS model behaviour compared to observations in the UTLS (above 10 km). The TTL base and top altitudes derived from the reference run are 14.2 and 18.6 km. This is consistent with the TTL characteristics derived from micro-SDLA data by Huret et al. (2006b)<sup>3</sup> which are 14.2 km for the base and 18 km for the top.

As for SF2, backward trajectories were calculated from the reference run outputs at the location of the SF4 flight. The modelled convective precipitation (Fig. 7b) is well located as illustrated by the comparison with TRMM accumulated rainrate (Fig. 2b). From the trajectory analysis, two layers are found and their characteristics are given in Table 4. In layer 1 (10–14.2 km), the reference run  $r_v$  and RHI are underestimated by the model mainly below 11 km. The 10–11 km layer is the transition between the very dry layer and a moist layer. The model fails to reproduce the observed very sharp transition. This is likely due to the vertical correlation in the model which does not allow extremely large variations along the vertical. The air mass sampled by SF4 in layer 1 comes from ascending air from lower levels leading to a moistening during the hours preceding the flight. This moistening effect related to the dynamics competes with the

## Water vapour modelling in the tropical UTLS

V. Marécal et al.

Title Page

Abstract

Introduction

Conclusions

References

Tables

Figures

◀

▶

◀

▶

Back

Close

Full Screen / Esc

Printer-friendly Version

Interactive Discussion

removal of water vapour by ice nucleation and subsequent growth and sedimentation. This microphysical process becomes dominant in the model above 13.6 km leading to a net decrease of water vapour mixing ratio. The analysis of the SF2 flight showed that the temperature errors in the BRAMS simulation have an impact on the model's ability to reproduce the water vapour observations. For SF4, the temperature error is weaker (Fig. 10b and Table 3) and its impact is only important in the 12.5–14.7 km layer as illustrated in Fig. 10c (green solid line). In this layer, using micro-SDLA temperature measurements and BRAMS  $r_v$  to calculate RHI leads to an increase of RHI consistent with the observations. This result shows that part of the RHI underestimation in layer 1 is due to temperature errors in the model. The complementary possible explanations are an insufficient moistening of this layer by air ascent and/or a too fast drying by ice formation.

In layer 2 (TTL, 14.2–18.6 km), the air mass does not show significant changes of water vapour during the preceding hours since it does not experience significant up-lifting or ice formation because of undersaturated conditions. The distribution of water vapour in the TTL depends on the dynamics. Below 15.2 km the trajectory analysis shows that the air originates from a relatively dry area located north-west of the flight track. In the 14.2–15.2 km layer, the BRAMS model is able to reproduce the observed shape and values for  $r_v$  and RHI. Between 15.2 and 16.6 km the air comes from the convective area north of Bauru. This air is more humid in terms of relative humidity than below because previously moistened by convection (see Figs. 2b and 7b). This effect becomes less important above 16 km altitude leading to the decrease of the BRAMS RHI between 16 and 16.6 km. Nevertheless, the BRAMS model is able to simulate the observed variations of  $r_v$  and RHI between 14.2 and 16.6 km meaning that the model dynamics are realistic and in particular the location of the convection. Above 16.6 km, the model water vapour variations are small leading to a negligible impact of the horizontal dynamics on the water vapour distribution. As for SF2, the BRAMS model initial state for  $r_v$  is fairly homogeneous above 17 km. The  $r_v$  field is not changed during the simulation since this layer is not affected by any air ascent or ice nucleation.

**Water vapour  
modelling in the  
tropical UTLS**

V. Marécal et al.

Title Page

Abstract

Introduction

Conclusions

References

Tables

Figures

◀

▶

◀

▶

Back

Close

Full Screen / Esc

Printer-friendly Version

Interactive Discussion

## 6 Conclusions

The objective of this paper is to evaluate the ability of the BRAMS mesoscale model to simulate the observed vertical variations of water vapour in the tropical UTLS. This evaluation is based on comparisons with in situ water vapour and temperature measurements but also comparisons with ECMWF analysis fields in order to show the potential benefits of a mesoscale model with respect to a global analysis. Water vapour and temperature measurements were gathered by the micro-SDLA instrument during the SF2 and SF4 HIBISCUS balloon flights. Both flights exhibit large variations of water vapour in the UTLS but also large differences are found between the two sets of measurements. In both flights, layers with large supersaturations with respect to ice are observed.

The measured fine scale vertical structures in the UTLS have a typical length of 1 km or less. This is why a 250 m vertical grid-spacing was used in the UTLS in the BRAMS. The ECMWF model having a  $\sim 1$  km vertical grid-spacing in the UTLS can only give a smooth picture of the observed variations of temperature and water vapour. Apart from the vertical resolution, the differences between the BRAMS reference simulation and ECMWF analysis are:

- the horizontal resolution: 20 km for BRAMS and  $\sim 50$  km for ECMWF,
- a more complete microphysical scheme in BRAMS giving the possibility of large supersaturations with respect to ice,
- the assimilation of data in the ECMWF analysis when available giving the possibility to take into account valuable recent meteorological information leading to an update of the atmospheric state compared to any forecast (from BRAMS or ECMWF).

Sensitivity simulations with BRAMS were run to evaluate the impact of the vertical resolution, horizontal resolution and microphysical scheme on the mesoscale model performances.

### Water vapour modelling in the tropical UTLS

V. Marécal et al.

Title Page

Abstract

Introduction

Conclusions

References

Tables

Figures

◀

▶

◀

▶

Back

Close

Full Screen / Esc

Printer-friendly Version

Interactive Discussion

**Water vapour  
modelling in the  
tropical UTLS**

V. Marécal et al.

Title Page

Abstract

Introduction

Conclusions

References

Tables

Figures

◀

▶

◀

▶

Back

Close

Full Screen / Esc

Printer-friendly Version

Interactive Discussion

The analysis of the results showed that the ECMWF analysis performs well compared to micro-SDLA measurements for temperature for both flights. This is related to the data assimilation system which improves significantly the temperature field. As already found in previous studies (e.g. Ovarlez et al. 2000), we showed that ECMWF analysis generally underestimates water vapour in the upper troposphere. In supersaturated layers, we pointed out that the microphysical scheme removes instantaneously the excess of water vapour with respect to ice leading to lower water vapour mixing ratios compared to observations. Very recently, Tompkins et al. (2005) tested a new parameterization that attempts to represent ice supersaturation and the homogeneous ice nucleation process in the ECMWF model. They showed that this new parameterization leads to a reduction of the upper troposphere dry bias. In undersaturated conditions below 10 km altitude, ECMWF analysis reproduces generally well micro-SDLA water vapour profile. This is because water vapour information from radiosoundings below 10 km is used in the assimilation system. This is also because in undersaturated conditions the water vapour distribution does not rely on the microphysics but depends on the dynamics that is also well constraint by data assimilation. Above 17 km altitude, ECMWF analysis is drier than micro-SDLA for both flights.

The mesoscale simulation with the BRAMS model provides a generally good estimation of the measured temperature profiles except in layers with large gradients or with small scale variations of the gradient which are not well captured. In particular, this leads to a difference of  $\sim 5$  K at the cold point tropopause between micro-SDLA and BRAMS for SF2. For SF4, the BRAMS statistical results for temperature are slightly worse than ECMWF analysis but similar to ECMWF 48 h forecast.

For water vapour and RHI (relative humidity with respect to ice saturation), the BRAMS model gives significantly better results than ECMWF analysis with a reduction of the RHI RMSE greater than 10% in both cases. This improvement is mainly due to the microphysical scheme in BRAMS which can give ice supersaturations and a progressive removal of water vapour by ice nucleation and subsequent growth and sedimentation. Nevertheless, the mesoscale model never exhibits very large ice su-

**Water vapour  
modelling in the  
tropical UTLS**

V. Marécal et al.

Title Page

Abstract

Introduction

Conclusions

References

Tables

Figures

◀

▶

◀

▶

Back

Close

Full Screen / Esc

Printer-friendly Version

Interactive Discussion

persaturations (max RHI  $\sim 130\%$ ) like those found in the micro-SDLA data (max RHI  $>150\%$ ). This can be explained by the fact that (i) measured highest supersaturations are likely to be a transient state just before ice nucleation occurs and (ii) the BRAMS microphysical scheme is a bulk type parameterization which is less precise than a spectral bin parameterization for thin cirrus simulation as shown by Khvorostyanov et al. (2006). The vertical fine scale structures of the water vapour profile measured in the TTL are generally well simulated by the BRAMS model partly thanks to the 250 m vertical grid-spacing chosen. The impact of the horizontal resolution is small for both case studies. Above 17 km altitude, the underestimation of water vapour by BRAMS is similar to ECMWF analysis since no mesoscale process affects the lower stratosphere in the BRAMS simulations.

From a trajectory analysis, it was shown that the water vapour variations in the model depend on the dynamical and thermodynamic processes experienced by the sampled air parcel. The profiles from two flights undergo a range of different dynamical processes as shown in Huret et al. (2006a<sup>2</sup>, b<sup>3</sup>, c<sup>4</sup>): uplifting from the mid and low troposphere, large scale transport associated with a front, isentropic transport from mid-latitude upper troposphere. The dynamical processes are dominant in undersaturated conditions. In near-saturated or supersaturated conditions the thermodynamic environment, i.e. the air temperature, plays a major role since it controls the ice nucleation process and consequently the dehydration. For instance, the sharp minimum of temperature at the cold point tropopause in SF2 is not captured by the model leading to a large underestimation of RHI. In supersaturated layers where the BRAMS temperature is close to micro-SDLA, the model water vapour profile is generally close to the observations showing the good quality of the model's microphysical parameterization. The origin of the temperature uncertainties found in BRAMS simulations and ECMWF forecasts were not investigated in the present study. Temperature being dependent on many processes (radiative, dynamic, thermodynamic and microphysical), a special work needs to be done on this issue.

The BRAMS mesoscale model is able to reproduce most of the vertical variations

of water vapour in the UTLS and to provide significantly better results compared to ECMWF analysis. But the two cases studied in this paper are not sufficient to fully evaluate the mesoscale model performances to simulate the UTLS water vapour. In particular, since only one measured profile was available per case study, it was not possible to follow the time evolution of the water vapour structures. This knowledge of the time evolution would help confirming our interpretation of the processes involved in the variations of water vapour. A larger set of data will be acquired during the SCOUT-AMMA field experiment that will take place in western Africa in 2006. Balloon-borne measurements of water vapour making use of  $\mu$ SDLA and Lyman alpha hygrometers will be coordinated with aircraft measurements at different altitudes. This will give the opportunity to obtain a more complete description of the time evolution of the dynamical, thermodynamic and microphysical processes driving the UTLS water vapour. Therefore, a more detailed analysis of the mesoscale model behaviour will be possible. Moreover, since February 2006, the number of vertical levels has been increased in the ECMWF model leading to a  $\sim 400$  m vertical grid-spacing in the UTLS. It will be interesting to evaluate the impact of this finer grid on the ECMWF analysis of water vapour in the UTLS. Also the availability of more accurate water vapour sensors in radiosounding systems will be a determinant tool in the understanding of the water vapour evolution in the UTLS. In particular, they will provide regular information that will possibly be assimilated in global models.

*Acknowledgements.* This modelling study is supported by funds from the 5th PCRD (HIBISCUS project) and the French Centre National de le Recherche Scientifique (Programme National de Chimie Atmosphérique). This work makes use of the RAMS model, which was developed under the support of the National Science Foundation (NSF) and the Army Research Office (ARO). BRAMS model development and maintenance is supported by Brazilian Funding Agency for Studies and Projects (FINEP). Computer ressources were provided by CINES (Centre Informatique National de l'Enseignement Supérieur), project pce2227.

**Water vapour  
modelling in the  
tropical UTLS**

V. Marécal et al.

Title Page

Abstract

Introduction

Conclusions

References

Tables

Figures

◀

▶

◀

▶

Back

Close

Full Screen / Esc

Printer-friendly Version

Interactive Discussion

## References

- Brewer, A. W.: Evidence for a world circulation provided by measurements of helium and water vapour distribution in the stratosphere, *Q. J. R. Meteorol. Soc.*, 75, 351–363, 1949.
- Di Donfrancesco, G., Cairo, F., Viterbini, M., Morbidini, R., Buontempo, C., Fierli, F., Cardillo, F., Snels, M., Liberti, G. L., and Di Paolo, F.: Cloud and aerosol detection by balloonborne lidars and backscatter-sondes in the UTLS during HIBISCUS campaign: optical and dynamical properties, *Geophys. Res. Abstracts*, 7, 03355, 2005.
- Durry, G. and Mégie, G.: Atmospheric CH<sub>4</sub> and H<sub>2</sub>O monitoring with near-infrared InGaAs laser diodes by the SDLA, a balloonborne spectrometer for tropospheric and stratospheric in situ measurements, *Appl. Opt.*, 38, 7342–7354, 1999.
- Durry, G. and Megie, G. : In situ measurements of H<sub>2</sub>O from a stratospheric balloon by diode laser direct-differential absorption spectroscopy at 1.39 μm, *Appl. Opt.*, 39, 5601–5608, 2000.
- Durry, G., Hauchecorne, A., Ovarlez, J., Ovarlez, H., Pouchet, I., Zeninari, V., and Parvitte, B.: In situ measurement of H<sub>2</sub>O and CH<sub>4</sub> with telecommunication laser diodes in the lower stratosphere: dehydration and indication of a tropical air intrusion at mid-latitudes, *J. Atmos. Chem.*, 43, 175–194, 2002.
- Durry, G., Danguy, T., and Pouchet, I.: Open two-mirror multipass absorption cell for in situ monitoring of stratospheric trace-gas with telecommunication laser diodes, *Appl. Opt.*, 41, 424–433, 2002.
- Durry, G., Amarouche, N., Zéninari, V., Parvitte, B., Le Barbu, T., and Ovarlez, J.: In situ sensing of the middle atmosphere with balloonborne near-infrared laser diodes, *Spectrochimica Acta, Part A*, 60, 3371–3379, 2004.
- Durry, G. and Hauchecorne, A.: Evidence for long-lived polar vortex air in the mid-latitude summer stratosphere from in situ laser diode CH<sub>4</sub> and H<sub>2</sub>O measurements, *Atmos. Chem. Phys.*, 5, 1467–1472, 2005.
- Durry, G., Zeninari, V., Parvitte, B., Le Barbu, T., Lefevre, F., Ovarlez, J., and Gamache, R. R.: Pressure-broadening coefficients and line strengths of H<sub>2</sub>O near 1.39 μm: application to the in situ sensing of the middle atmosphere with balloonborne diode lasers, *J. Quant. Spectrosc. Radiat. Transfer*, 94(3–4), 387–403, 2005.
- Folkens, I., Loewenstein, M., Podolske, J., Oltmans, S., and Proffitt, M.: A barrier to vertical mixing at 14 km in the tropics: Evidence from ozonesondes and aircraft measurements, *J.*

### Water vapour modelling in the tropical UTLS

V. Marécal et al.

Title Page

Abstract

Introduction

Conclusions

References

Tables

Figures

◀

▶

◀

▶

Back

Close

Full Screen / Esc

Printer-friendly Version

Interactive Discussion

- Geophys. Res., 104, 22 095–22 102, 1999.
- Freitas S. R., Silva Dias, M. A. F., Silva Dias, P. L., Longo, K. M., Artaxo, P., Andreae, M. O., and Fischer, H.: A convective kinematic trajectory technique for low-resolution atmospheric models, *J. Geophys. Res.*, 105, 24 375–24 386, 2000.
- 5 Freitas, S., Longo, K., Silva Dias, M., Silva Dias, P., Chatfield, R., Prins, E., Artaxo, P., Grell G., and Recuero, F.: Monitoring the transport of biomass burning emissions in South America. *Environmental Fluid Mechanics*, 5(1–2), 135–167, doi:10.1007/s10652-005-0243-7, 2005.
- Fujiwara, M., Shiotani, M., Hasebe, F., Vömel, H., Oltmans, S., Ruppert, P. W., Horinouchi, T., and Tsuda T.: Performance of the meteorolabor “Snow White” chilled-mirror hygrometer in the  
10 tropical troposphere: Comparisons with the Vaisala RS80 A/H-Humicap sensors, *J. Atmos. Ocean. Technol.*, 20, 1534–1542, 2003.
- Gettelman, A., Randel, W. J., Wu, F., and Massie, S. T.: Transport of water vapour in the tropical tropopause layer, *Geophys. Res. Lett.*, 29, 1009, doi:10.1029/2001GL013818, 2002.
- 15 Gevaerd, R. and Freitas, S.: Estimativa operacional da umidade do solo para inicio de modelos de previso numerica da atmosfera. Parte 1: descricio da metodologia e validao, *Brazilian J. Meteorol.*, LBA Special Issue, in press, 2006.
- Grell, G. A. and Devenyi, D.: A generalized approach to parameterizing convection combining ensemble and data assimilation techniques, *Geophys. Res. Lett.*, 29, 1693, doi:10.1029/2002GL015311, 2002.
- 20 Highwood, E. J. and Hoskins, B. J.: The tropical tropopause, *Q. J. R. Meteorol. Soc.*, 124, 1579–1604, 1998.
- Hintsä, E., Weinstock, E. M., Anderson, J. G., May, R. D., and Hurst, D. F.: On the accuracy of in situ water vapour measurements in the troposphere and lower stratosphere with the Harvard Lyman- $\alpha$  hygrometer, *J. Geophys. Res.*, 104, 8183–8190, 1999.
- 25 Jensen, E. and Pfister, L.: Transport and freeze-drying in the tropical tropopause layer, *J. Geophys. Res.*, 108, D02207, doi:10.1029/2003JD004022, 2004.
- Jensen, E., Pfister, L., Bui, T., Weinheimer, A., Weinstock, E., Smith, J., Pittman, J., Baumgardner, D., Lawson, P., and McGill, J.: Formation of a tropopause cirrus layer observed over Florida during CRYSTAL-FACE, *J. Geophys. Res.*, 110, D03208, doi:10.1029/2004JD004671, 2005a.
- 30 Jensen, E., Smith, J., Pfister, L., Pittman, J., L., Weinstock, E., Sayres, D. S., Herman, R. L., Troy, R. F., Rosenlof, K., Thompson, T. L., Fridlind, A. M., Hudson, P. K., Cziczko, D. J., Heysfield, A. J., Schmitt, C., and Wilson, J.C.: Ice supersaturations exceeding 100% at the

---

**Water vapour  
modelling in the  
tropical UTLS**V. Marécal et al.

---

[Title Page](#)[Abstract](#)[Introduction](#)[Conclusions](#)[References](#)[Tables](#)[Figures](#)[◀](#)[▶](#)[◀](#)[▶](#)[Back](#)[Close](#)[Full Screen / Esc](#)[Printer-friendly Version](#)[Interactive Discussion](#)

cold tropical tropopause: implications for cirrus formation and dehydration, *Atmos. Chem. Phys.*, 5, 851–862, 2005b.

Khvorostyanov, V. I., Morrison, H., Curry, J. A., Baumgardner, D., and Lawson, P.: High supersaturation and modes of ice nucleation in thin tropopause cirrus: Simulation of the 13 July 2002 Cirrus Regional Study of Tropical Anvils and Cirrus Layers case, *J. Geophys. Res.*, 111, D02201, doi:10.1029/2004JD005235, 2006.

May, R. D.: Open path near-infrared tunable diode laser spectrometer for atmospheric measurements of H<sub>2</sub>O, *J. Geophys. Res.*, 103, 19 161–19 172, 1998.

Miloshevich, L. M., Vömel, H., Paukkunen, A., Heymsfield, A. J., and Oltmans, S. J.: Characterization and correction of relative humidity measurements from Vaisala RS-80-A radiosondes at cold temperatures, *J. Atmos. Ocean. Technol.*, 18, 135–156, 2001.

Offermann, D., Schaeler, B., Riese, M., Langfermann, M., Jarisch, M., Eidmann, G., Schiller, C., Smit, H.G.J., and Read, W.G.: Water vapor at the tropopause during the CRISTA 2 mission, *J. Geophys. Res.*, 107(D23), 8176, doi:10.1029/2001JD000700, 2002.

Ovarlez, J. and Van Velthoven, P.: Comparison of water vapour measurements with data retrieved from ECMWF analyses during the POLINAT experiment, *J. Appl. Meteorol.*, 36, 1329–1335, 1997.

Ovarlez, J., Van Velthoven, P., Sachse, G., Vay, S., Schlager, H., and Ovarlez, H.: Comparison of water vapour measurements from POLINAT 2 with ECMWF analyses in high-humidity conditions, *J. Geophys. Res.*, 105, 3737–3744, 2000.

Ovarlez, J., Gayet, J.-F., Gierens, K., Ström, J., Ovarlez, H., Auriol, F., Busen., R., and Schumann, U.: Water vapour measurements inside cirrus clouds in northern and southern hemispheres during INCA, *Geophys. Res. Lett.*, 29, 1813, doi:10.1029/2001GL014440, 2002.

Parvitte B., Zeninari, V., Pouchet, I., and Durry, G.: Diode laser spectroscopy of H<sub>2</sub>O in the 7165–7185 cm<sup>-1</sup> range for atmospheric applications, *J. Quant. Spectros. Radiat. Transfer*, 75, 493–507, 2002.

Sonntag, D.: The history of formulations and measurements of ice pressure, In proceedings of the 3rd Int. Symposium on Humidity and Moisture, National Physical Laboratory, UK, 93–102, 1998.

Spichtinger, P., Gierens, K., and Wernli, H.: A case study on the formation and evolution of ice supersaturation in the vicinity of a warm conveyor belt's outflow region, *Atmos. Chem. Phys.*, 5, 973–987, 2005.

Tompkins, A. M., Gierens, K., and Rädcl, G.: Ice supersaturation in the ECMWF Integrated

**Water vapour  
modelling in the  
tropical UTLS**

V. Marécal et al.

Title Page

Abstract

Introduction

Conclusions

References

Tables

Figures

◀

▶

◀

▶

Back

Close

Full Screen / Esc

Printer-friendly Version

Interactive Discussion

Forecast System, ECMWF Technical Memorandum, 481, 2005.

Turner, D. D., Lesht, B. M., Clough, S. A., Liljegren, J. C, Revercomb, H. E., and Tobin, D. C.: Dry bias and variability in Vaisala RS80-H Radiosondes: The ARM experience, *J. Atmos. Ocean. Technol.*, 20, 117–132, 2003.

5 Vömel, H., Oltmans, S. J., Johnson, B. J., Hasebe, F., Shiotani, M., Fujiwara, M., Nishi, N., Agama, M., Cornejo, J., Paredes, F., and Enriquez, H.: Balloon-borne observations of water vapor and ozone in the tropical upper troposphere and lower stratosphere, *J. Geophys. Res.*, 107(D14), 4210, doi:10.1029/2001JD000707, 2002.

Walko, R. L., Cotton, W. R., Meyers, M. P., and Harrington, J. Y.: New RAMS cloud microphysics parameterization. Part I: the single-moment scheme, *Atmos. Res.*, 38, 29–62, 1995.

10 Walko, R., Band, L., Baron J., Kittel, F., Lammers, R., Lee, T., Ojima, D., Pielke, R., Taylor, C., Tague, C., Tremback, C., and Vidale, P.: Coupled atmosphere-biophysics-hydrology models for environmental modeling, *J. Appl. Meteorol.* 39, 6, 931–944, 2000.

15 Zöger, M., Afchine, A., Eicke, N., Gerhards, M. T., Klein, E., McKenna, D. S., Mörschel, U., Schmidt, U., Tan, V., Tuitjet, F., Woyke, T., and Schiller, C.: Fast in situ stratospheric hygrometers: A new family of balloonborne and airborne Lyman-alpha photofragment fluorescence hygrometers, *J. Geophys. Res.*, 104, 1807–1816, 1999.

---

**Water vapour  
modelling in the  
tropical UTLS**

V. Marécal et al.

---

Title Page

Abstract

Introduction

Conclusions

References

Tables

Figures

◀

▶

◀

▶

Back

Close

Full Screen / Esc

Printer-friendly Version

Interactive Discussion

## Water vapour modelling in the tropical UTLS

V. Marécal et al.

**Table 1.** Statistical results for SF2 flight: correlation and RMSE (Root Mean Square Error) between the model (ECMWF or BRAMS) and micro-SDLA averaged over the corresponding model grid.

	temperature RMSE (K)	RHI correlation	RHI RMSE (%)
ECMWF analysis	1.69	0.905	26.5
ECMWF 48 h forecast started on 12 Feb 2004 at 00:00 UTC	1.84	0.827	36.4
Run with 1 km vertical resolution	1.60	0.975	17.7
Reference run	1.76	0.960	15.7
Run with 50 km horizontal resolution	1.72	0.953	17.5
Run with 5 km resolution	1.84	0.968	13.2
(2 grids)			
Run with simplified microphysics	1.85	0.902	33.6

Title Page

Abstract

Introduction

Conclusions

References

Tables

Figures

◀

▶

◀

▶

Back

Close

Full Screen / Esc

Printer-friendly Version

Interactive Discussion

## Water vapour modelling in the tropical UTLS

V. Marécal et al.

**Table 2.** Characteristics of the three layers identified from the SF2 trajectory analysis based on the BRAMS reference simulation above 10 km altitude.

	Altitude range (km)	Air mass origin vert./horiz.	Moisture tendency	Ice formation during previous hours
Layer 1	10–13.7	Upper and mid-troposphere/South-west	drying	yes
Layer 2	13.7–17.3	TTL/North-west at 13.7 km changing to TTL/South east with increasing altitude	drying below 14.3 km and constant above	yes only below 14.3 km
Layer 3	Above 17.3	Stratosphere/East	constant	no

Title Page

Abstract

Introduction

Conclusions

References

Tables

Figures

◀

▶

◀

▶

Back

Close

Full Screen / Esc

Printer-friendly Version

Interactive Discussion

## Water vapour modelling in the tropical UTLS

V. Marécal et al.

**Table 3.** Same as Table 1 but for SF4 flight.

	temperature RMSE (K)	RHI correlation	RHI RMSE (%)
ECMWF analysis	0.80	0.801	48.5
ECMWF 48 h forecast started on 23 Feb 2004 at 00:00 UTC	1.15	0.615	63.7
Run with 1 km vertical resolution	1.19	0.673	35.9
Reference run	1.26	0.797	29.6
Run with 50 km horizontal resolution	1.29	0.779	31.0
Run with 5 km resolution (2 grids)	1.45	0.793	31.7
Run with simplified microphysics	1.63	0.510	74.7

Title Page

Abstract

Introduction

Conclusions

References

Tables

Figures

◀

▶

◀

▶

Back

Close

Full Screen / Esc

Printer-friendly Version

Interactive Discussion

## Water vapour modelling in the tropical UTLS

V. Marécal et al.

**Table 4.** Characteristics of the two layers identified from the SF4 trajectory analysis based on the BRAMS reference simulation above 10 km altitude.

	Altitude range (km)	Air mass origin vertical/horizontal	Moisture tendency	Ice formation during previous hours
Layer 1	10–14.2	Mid-troposphere/ North-west	Moistening below 13.6 km and drying above	Yes above 11 km and increasing with altitude
Layer 2	14.2–18.6	TTL/North-west between 14.2 and 15.2 km Above 15.2 km TTL/North changing to East with increasing altitude	Constant	No

[Title Page](#)
[Abstract](#)
[Introduction](#)
[Conclusions](#)
[References](#)
[Tables](#)
[Figures](#)
[Back](#)
[Close](#)
[Full Screen / Esc](#)
[Printer-friendly Version](#)
[Interactive Discussion](#)

**Water vapour  
modelling in the  
tropical UTLS**

V. Marécal et al.

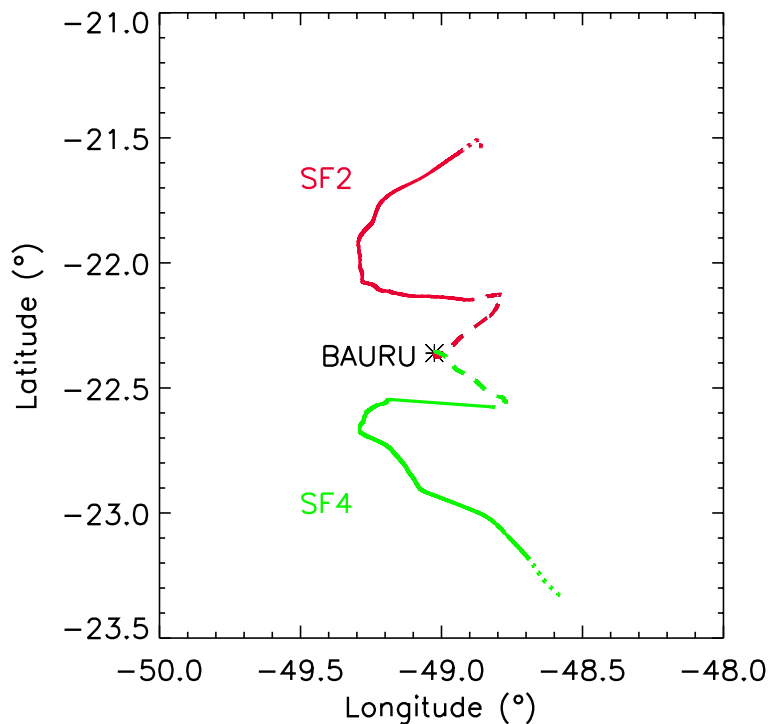


**Fig. 1.** Projection on the horizontal plan of the trajectory of the SF2 and SF4 balloon flights. The dashed, solid and dotted lines correspond respectively to the ascent, slow descent and rapid descent after cut down of the balloon. The red lines correspond to SF2 and green lines to SF4.

[Title Page](#)[Abstract](#)[Introduction](#)[Conclusions](#)[References](#)[Tables](#)[Figures](#)[◀](#)[▶](#)[◀](#)[▶](#)[Back](#)[Close](#)[Full Screen / Esc](#)[Printer-friendly Version](#)[Interactive Discussion](#)

**Water vapour  
modelling in the  
tropical UTLS**

V. Marécal et al.

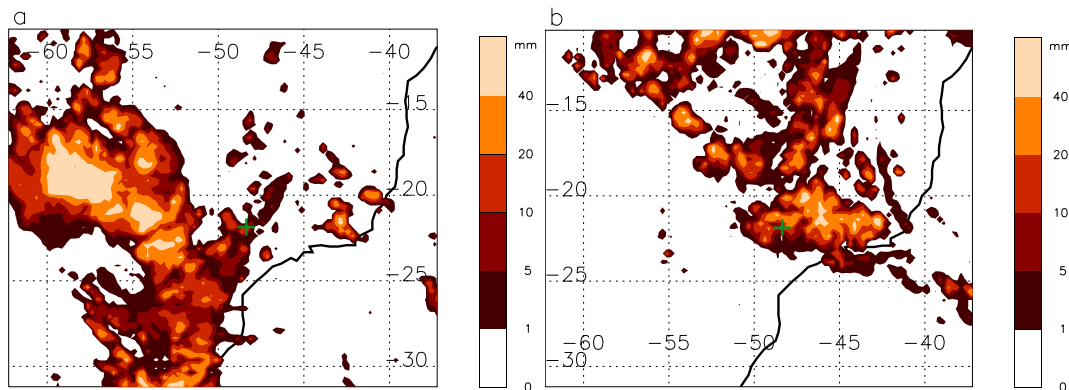


**Fig. 2.** Accumulated TRMM rainfall in mm **(a)** from 19:30 UTC on 13 February 2004 to 10:30 UTC on 14 February 2004 and **(b)** from 16:30 UTC on 24 February 2004 to 04:30 UTC on 25 February 2004. The green cross corresponds to the location of Bauru balloon launch site. The area plotted in these figures corresponds to the domain used in the BRAMS simulations.

[Title Page](#)[Abstract](#)[Introduction](#)[Conclusions](#)[References](#)[Tables](#)[Figures](#)[◀](#)[▶](#)[◀](#)[▶](#)[Back](#)[Close](#)[Full Screen / Esc](#)[Printer-friendly Version](#)[Interactive Discussion](#)

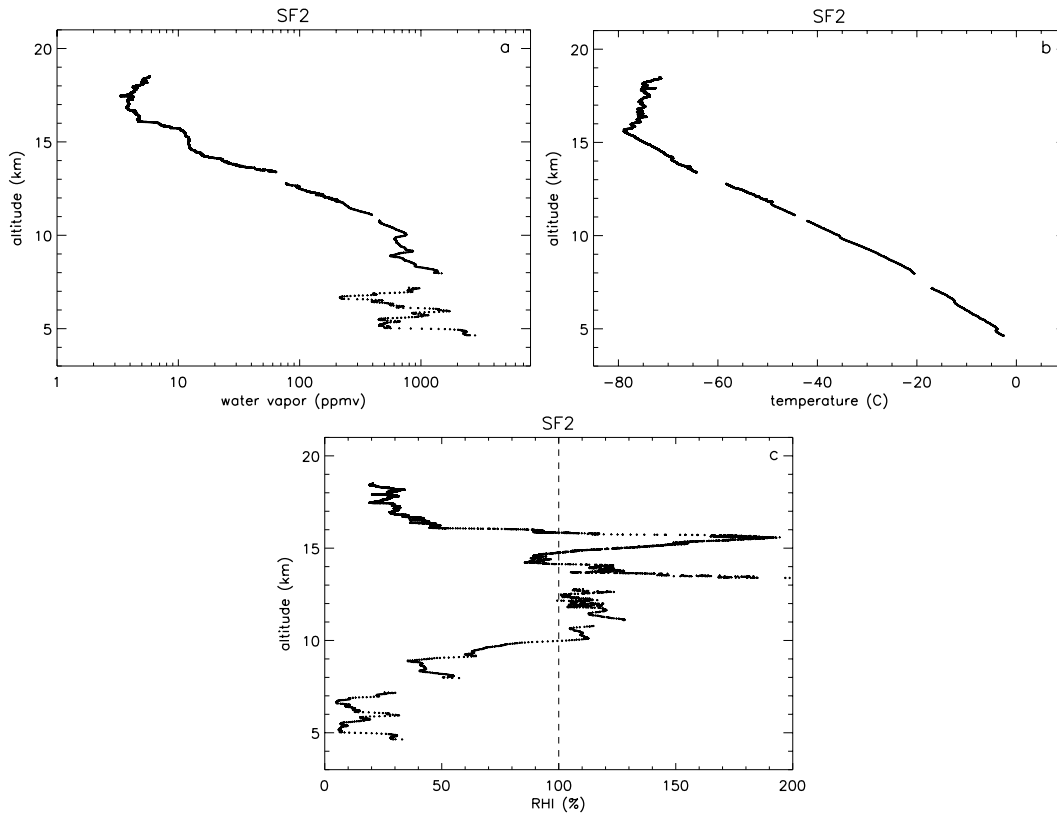


**Fig. 3.** SF2 flight: **(a)** water vapour mixing ratio in ppmv from micro-SDLA measurements, **(b)** temperature in °C from micro-SDLA measurements, **(c)** derived relative humidity with respect to ice saturation (RHI) in %.

**Water vapour  
modelling in the  
tropical UTLS**

V. Marécal et al.

Title Page

Abstract

Introduction

Conclusions

References

Tables

Figures

◀

▶

◀

▶

Back

Close

Full Screen / Esc

Printer-friendly Version

Interactive Discussion

**Water vapour  
modelling in the  
tropical UTLS**

V. Marécal et al.

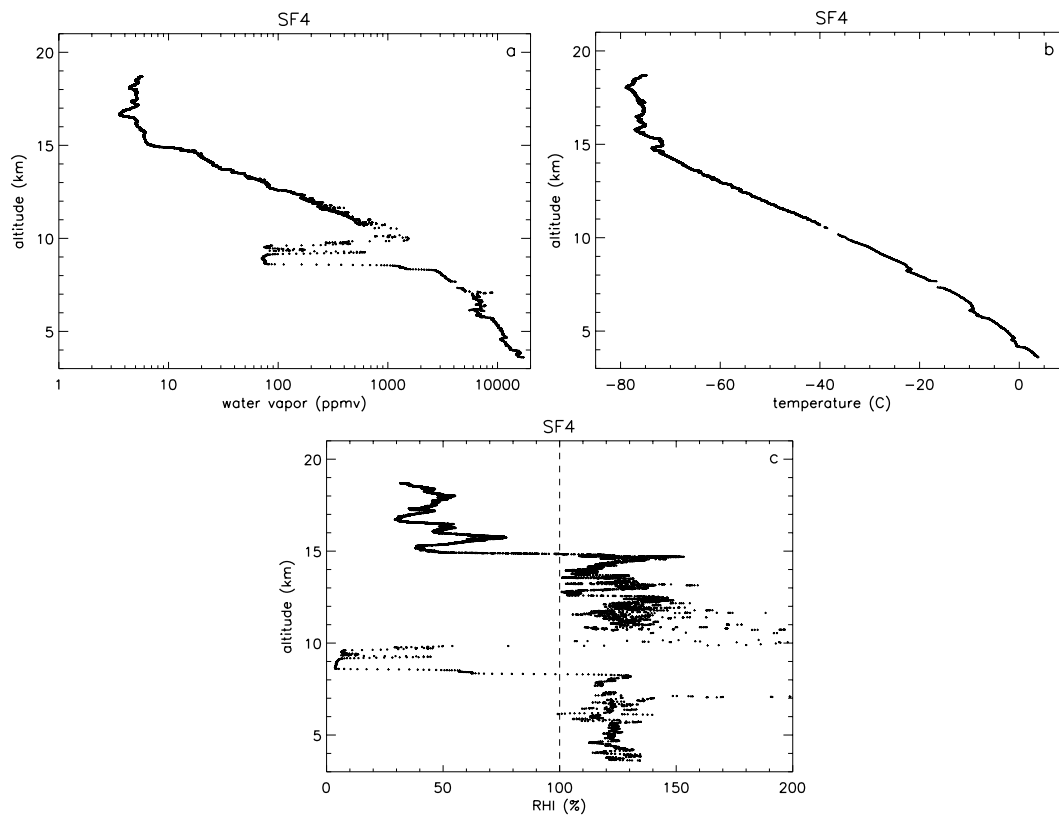


**Fig. 4.** Same as Fig. 3 but for SF4 flight measurements.

[Title Page](#)[Abstract](#)[Introduction](#)[Conclusions](#)[References](#)[Tables](#)[Figures](#)[◀](#)[▶](#)[◀](#)[▶](#)[Back](#)[Close](#)[Full Screen / Esc](#)[Printer-friendly Version](#)[Interactive Discussion](#)

Water vapour  
modelling in the  
tropical UTLS

V. Marécal et al.

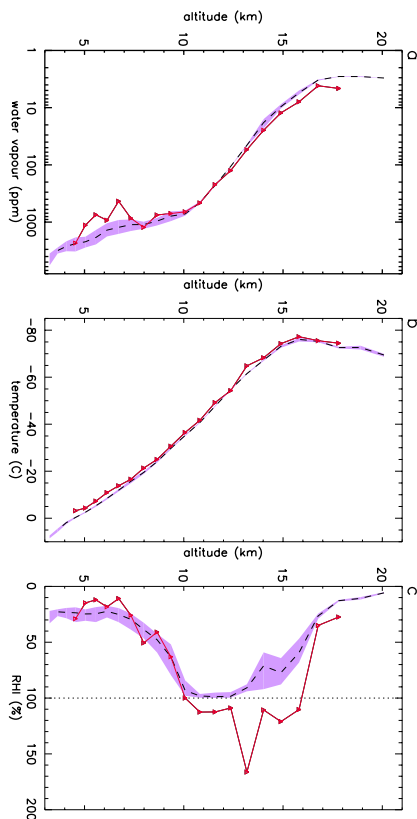


**Fig. 5.** Comparison between ECMWF analysis and micro-SDLA SF<sub>2</sub> measurements **(a)** for water vapour in ppmv, **(b)** for temperature in °C and **(c)** for RH in %. The micro-SDLA data are averaged on the ECMWF model vertical grid and shown as a solid red line with the triangles showing the model levels. The black dashed line and the purple area show, respectively, the mean and the minimum/maximum for a set of selected model profiles. Details on the selected profiles are given in the text.

[Title Page](#)[Abstract](#)[Introduction](#)[Conclusions](#)[References](#)[Tables](#)[Figures](#)[◀](#)[▶](#)[◀](#)[▶](#)[Back](#)[Close](#)[Full Screen / Esc](#)[Printer-friendly Version](#)[Interactive Discussion](#)

Water vapour  
modelling in the  
tropical UTLS

V. Marécal et al.

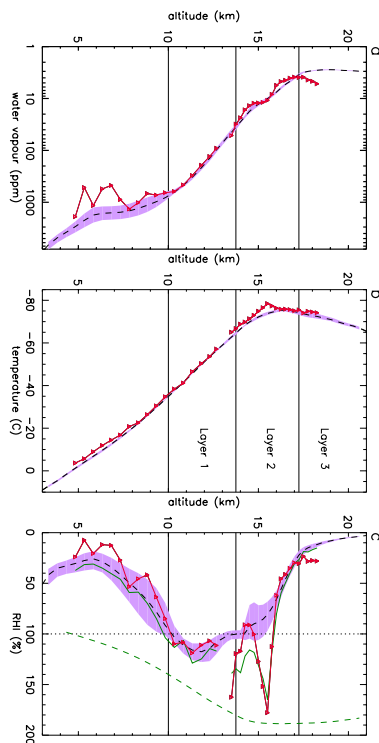


**Fig. 6.** Comparison between BRAMS reference simulation and micro-SDLA SF2 measurements **(a)** for water vapour in ppmv, **(b)** for temperature in °C and **(c)** for RHI in %. The micro-SDLA data are averaged on the BRAMS model vertical grid and shown as a solid red line with the triangles showing the model levels. The black dashed line and the purple area show, respectively, the mean and the minimum/maximum for a set of selected model profiles. Details on the selected profiles are given in the text. In (c), the green solid line corresponds to RHI calculated using  $r_v$  from the BRAMS reference run and the micro-SDLA temperature. The green dashed line corresponds to 100% saturation with respect to liquid water calculated using BRAMS mean temperature profile.

[Title Page](#)[Abstract](#)[Introduction](#)[Conclusions](#)[References](#)[Tables](#)[Figures](#)[◀](#)[▶](#)[◀](#)[▶](#)[Back](#)[Close](#)[Full Screen / Esc](#)[Printer-friendly Version](#)[Interactive Discussion](#)

Water vapour  
modelling in the  
tropical UTLS

V. Marécal et al.

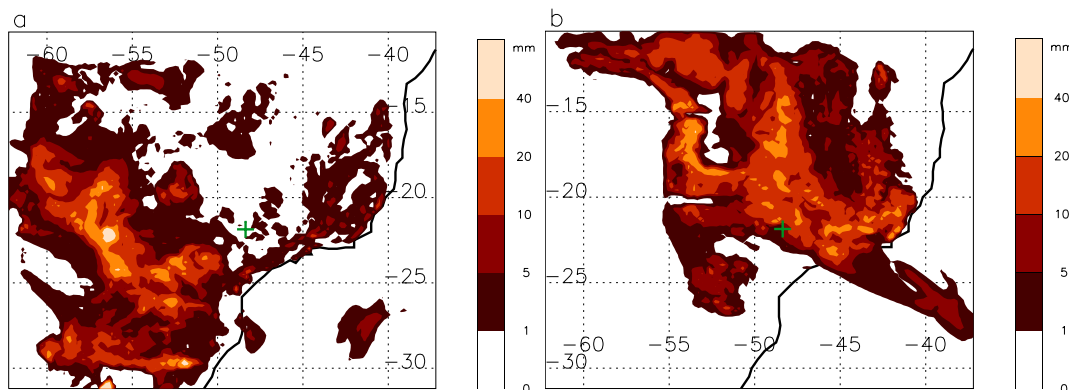
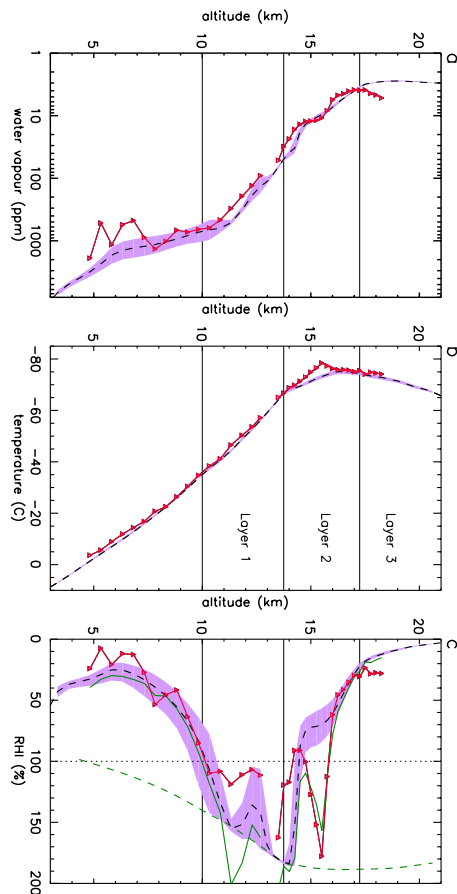


**Fig. 7.** Accumulated rainfall rate from the reference run in mm **(a)** from 19:30 UTC on 13 February 2004 to 10:30 UTC on 14 February 2004 and **(b)** from 16:30 UTC on 24 February 2004 to 04:30 UTC on 25 February 2004. The green cross corresponds to the location of Bauru balloon launch site.

[Title Page](#)[Abstract](#)[Introduction](#)[Conclusions](#)[References](#)[Tables](#)[Figures](#)[◀](#)[▶](#)[◀](#)[▶](#)[Back](#)[Close](#)[Full Screen / Esc](#)[Printer-friendly Version](#)[Interactive Discussion](#)

Water vapour  
modelling in the  
tropical UTLS

V. Marécal et al.

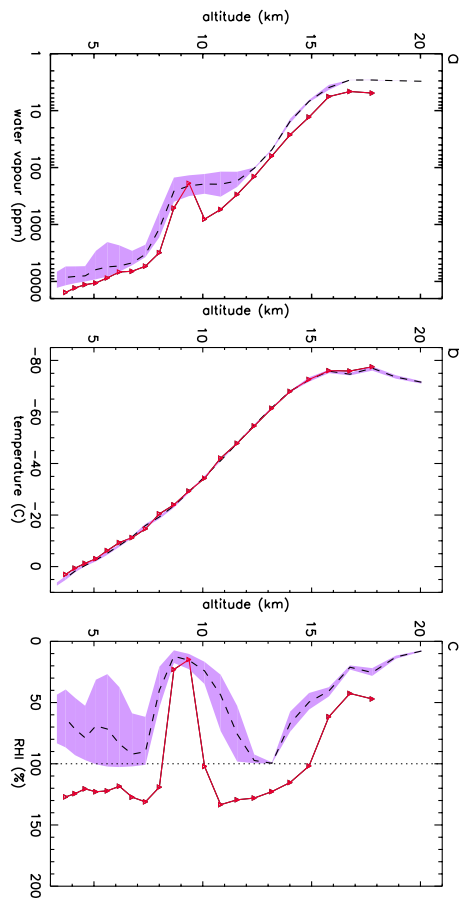


**Fig. 8.** Same as Fig. 6 but for the BRAMS sensitivity run with simplified microphysics (see text for details on this run).

[Title Page](#)[Abstract](#)[Introduction](#)[Conclusions](#)[References](#)[Tables](#)[Figures](#)[◀](#)[▶](#)[◀](#)[▶](#)[Back](#)[Close](#)[Full Screen / Esc](#)[Printer-friendly Version](#)[Interactive Discussion](#)

**Water vapour  
modelling in the  
tropical UTLS**

V. Marécal et al.

**Fig. 9.** Same as Fig. 5 but for SF4.

Title Page

Abstract

Introduction

Conclusions

References

Tables

Figures

◀

▶

◀

▶

Back

Close

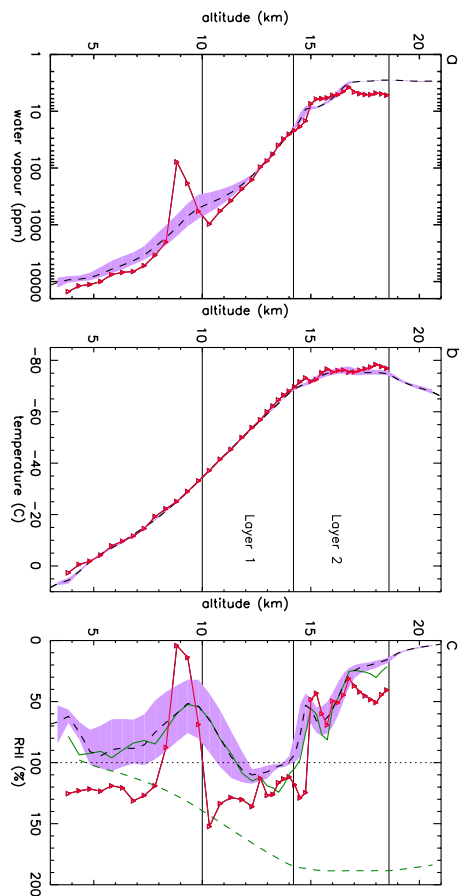
Full Screen / Esc

Printer-friendly Version

Interactive Discussion

**Water vapour  
modelling in the  
tropical UTLS**

V. Marécal et al.

**Fig. 10.** Same as Fig. 6 but for SF4.

Title Page

Abstract

Introduction

Conclusions

References

Tables

Figures

◀

▶

◀

▶

Back

Close

Full Screen / Esc

Printer-friendly Version

Interactive Discussion